

Excitation of whispering-gallery modes with a fiber-based optical antenna

Stephy Vincent,¹ Fuchuan Lei,^{1, a)} Jonathon M. Ward,¹ Samir K Mondal,² Pooja Gupta,^{2, 3} Jochen Fick,⁴ and Sile Nic Chormaic^{1, 4}

¹⁾ *Light-Matter Interactions Unit, Okinawa Institute of Science and Technology Graduate University, Onna, Okinawa 904-0495, Japan*

²⁾ *CSIR-Central Scientific Instruments Organisation, Chandigarh, Sec.-30C, India*

³⁾ *Academy of Scientific and Innovative Research (AcSIR), Ghaziabad, India*

⁴⁾ *Universit Grenoble Alpes, CNRS, Grenoble INP, Institut Nel, 38000 Grenoble, France*

(Dated: 19 May 2022)

We demonstrate the excitation and detection of whispering-gallery modes (WGMs) in optical microresonators using a fiber-based optical antenna. The coupling mechanism is based on cavity-enhanced Rayleigh scattering. The collected spectra exhibit either Lorentz dips, Fano shapes, or Lorentz peaks. The coupling method is simple, low-cost and, most importantly, it does not reduce the quality (Q) factors of the cavity modes, thereby making it particularly suitable for metrology, sensing applications, or cavity quantum electrodynamics (cQED) experiments.

The past decades have seen intense research efforts for the development of whispering gallery (WG) microresonators using different materials and geometries¹. The combination of the extremely high optical quality (Q) factor and small mode volume makes WG resonators especially suitable for studying lasing behavior^{2,3}, nonlinear optics⁴, quantum optics⁵, optical information processing⁶, optomechanics⁷, sensing^{8,9}, fundamental physics¹⁰ etc.

In order to take WG resonators out of the research laboratory environment and increase their functionality for real-world applications, it is critical that researchers find a simpler way to couple light into and out of the resonator. In general, free-space beams cannot be used to excite high Q-factor modes efficiently due to phase mismatching¹ between the beam and the cavity modes. This limitation can be overcome by introducing cavity deformation, thereby allowing chaotic rays to assist in the coupling¹¹. Alternatively, the phase-matching condition can be satisfied by using evanescent wave coupling, achieved via, for example, a prism¹², a side-polished fiber¹³, or a tapered fiber¹⁴. A high coupling efficiency from the near-field interaction is achievable, but these each have their own disadvantages; the prism method is limited by its bulky size, while it is difficult to satisfy the phase-matching condition for side-polished fibers. For this reason, the tapered optical fiber coupling technique is widely used because it provides a fiber-integrated solution to the coupling problem and near-ideal coupling is attainable¹⁴. However, once more there are limitations with this popular technique. For example, the length of the tapered regions cannot be arbitrarily short since the adiabatic condition for efficient mode propagation must be satisfied¹⁵; this leads to tapered fibers being fairly fragile during their use. Previous works have demonstrated packaging of the tapered fiber and microresonator

into glue or low refractive index materials^{16–18} to overcome this problem; however, the cavity Q-factors inevitably decrease by such modifications. Another drawback of such a packaging method is that the resulting device has two pigtailed, i.e., one input and one output port, making the system somewhat cumbersome.

In recent years, there have been several attempts at injecting light into, and collecting light from, whispering gallery resonators using single-ended waveguides, including on-chip^{19–21} and fiber-based configurations^{22,23}. However, the presence of the waveguide considerably modifies the geometry of the system and, as a result, high-Q factor modes cannot be maintained and they are limited to about 10^5 . Very recently, an interesting single-ended waveguide configuration was demonstrated by Shu *et al.*²⁴; they placed a small Rayleigh scatterer, which acts as a nano-antenna, on the surface of the microsphere. A light beam was focused onto the antenna using a graded-index (GRID) fiber-coupled lens. Thence, they demonstrated light coupling between the free-space beam and the WG modes. Here, the collected light was in the far-field and coupled back into the launching fiber. Due to the Purcell effect^{25–27}, a coupling efficiency of 16.8% was achieved. Even though feasible, this configuration relied on a commercial GRID lens and tricky alignment. At this point, it is worthwhile noting that WG modes can be directly mapped using a fiber-based optical nano-antenna, i.e., a near-field probe²⁸. However, to date, there is no report on complete use of both illumination and collection modes using the fiber-based antenna for WG microresonators.

In this work, we propose and demonstrate an alternative whispering gallery resonator coupling scheme that is both easy to make and requires very little alignment. We show that a fiber-based optical nano-antenna²⁹ can be used to *simultaneously* excite and collect light from the WG modes (WGM) of a silica microsphere. The coupling proves to be both very convenient and stable, and the Q-factors of the modes can be maintained at values higher than 10^8 . The maximum input/output efficiency that we

^{a)} Electronic mail: fuchuan.lei@oist.jp

can reach using this coupling technique is as high as 1.8%. This fiber-based antenna is the first single-ended high-Q maintaining coupler for WGM resonators and shows interesting features, making it very promising for optical sensing applications or for achieving strong coupling with quantum emitters.

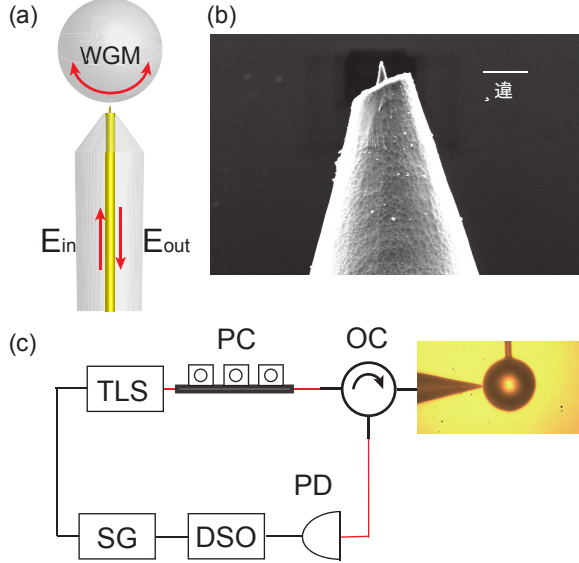


FIG. 1. (a) Schematic of the coupling system. (b) SEM image of the fiber-based nano-antenna. (c) Experimental setup. PC: Polarization controller; TLS: Tunable laser; OC: Optical circulator; PD: Photodiode; DSO: Digital signal oscilloscope; SG: signal generator; WGM: whispering gallery mode.

Figure 1(a) shows the schematic of the coupling system. A fiber-based optical antenna is brought into the evanescent field of a spherical WGM resonator. A scanning electron microscope (SEM) image of the fiber-based optical antenna is given in Fig. 1(b). The antenna was developed on the tip of a highly Germanium-doped single-mode optical fiber by etching in 48% hydrofluoric acid solution in a hydrophobic capillary tube. The etching process simply exploits surface tension and capillary action, an interaction between contacting surfaces of a liquid and a solid, and different etching rates for the Germanium-doped optical fiber core and cladding materials. Full details of the fabrication process can be found in^{29,30}. The end-face of the antenna has a curvature with a typical radius of 50 nm. The microsphere resonator is fabricated from standard silica fiber using a CO₂ laser⁶. The diameters of microspheres used in this work range from 50 μm to 200 μm .

Light incident on the microsphere can excite WGMs that travel in both the clockwise (CW) and counterclockwise (CCW) directions via Rayleigh scattering from the optical antenna²⁶. At the same time, some of the light can be coupled back into the fiber pigtail through the optical antenna. A schematic diagram of the experiment setup is presented in Fig. 1(c). We use a tunable laser

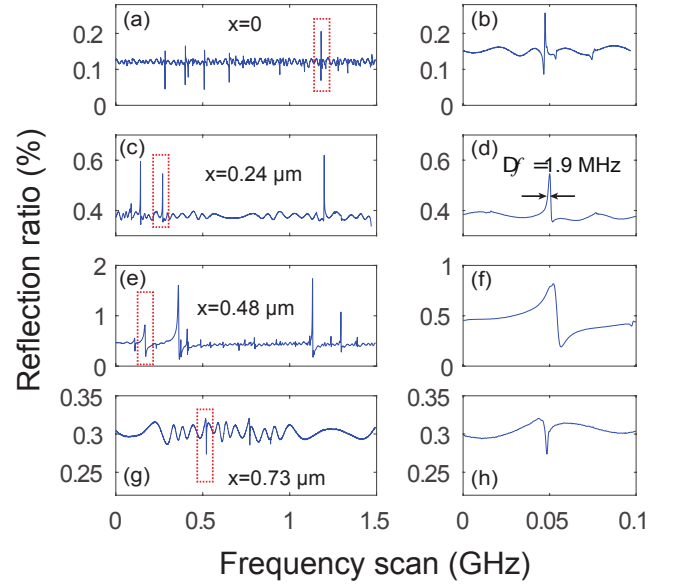


FIG. 2. The normalized spectra of the reflected signal when the fiber-based antenna is used for excitation of resonances in a 186 μm diameter silica microsphere. From top to bottom the gaps between the antenna and the microsphere are (a)&(b) 0; (c)&(d) 0.24 μm , (e)&(f) 0.48 μm , and (g)&(h) 0.73 μm . The plots on the right-hand side are zoomed in regions of those on the left, as indicated by the red boxes. The small fluctuation of the base line is the laser noise.

(Newport TLB 6700) in the 1592 nm wavelength range for this work. A fiber polarization controller (PC) is used to control the polarization of the incident field and an optical circulator (OC) facilitates both excitation of, and collection from, the WGM modes. The reflected signal is monitored on a photodiode (PD). The microsphere was kept fixed during experiments, whereas the movement of the antenna is controlled using a three-dimensional nanostage (SmarAct GmbH, MCS-3D).

The measured signals are presented in Fig. 2. From top to bottom, the gap between the antenna and microsphere increases from 0 to 0.73 μm (this gap difference is marked as x in the figure). It is interesting to note that there are two clear effects occurring with a change in gap size: (i) the base line changes and (ii) the narrow lineshape, which corresponds to the cavity modes, also changes, e.g., from Fano to Lorentz peaks, as well as dips. This latter phenomenon can be explained as an interference between two back-coupled fields through the fiber¹⁹. One field is a direct reflection from the surface of the microsphere, whereas the other is the field scattered from the cavity modes by the antenna. Hence, the total reflected field, E_{out} , is composed of two parts, i.e.,

$$E_{\text{out}} = r e^{i\theta} E_{\text{in}} + \frac{2\kappa E_{\text{in}}}{i(\omega - \omega_0) - \gamma}, \quad (1)$$

where $r e^{i\theta}$ is the reflection coefficient, θ is the phase change between the input and output fields, κ is the coupling loss caused by the antenna, ω_0 is the resonant fre-

quency, and γ is the total decay ratio of the cavity mode, corresponding to a cavity quality factor $Q = \omega/2\gamma$. Both the coupling loss and the reflection coefficient are dependent on the gap between the antenna and resonator. The reflected field is negligible when the antenna is far away from the sphere since the evanescent wave diminishes significantly with distance from the tip surface³¹. Note that the field reflected from the surface of the sphere corresponds to a continuum spectrum, while the scattered cavity field corresponds to a discrete spectrum. As a result, Fano lineshapes are formed³².

Besides the spectral dependence on the gap, we also find that the reflection spectra rely on the input polarization, as shown in Fig. 3. This phenomenon can be understood if we consider the following two points: (i) the fabricated antenna is not rotationally symmetric; therefore, the transmittance through the antenna depends on the polarization and (ii) the excitation of WGMs depends on the polarization of the excitation light. In general, we can assume that the angular momentum of light from the nano-antenna includes both longitudinal and transversal spin components, and may even contain some orbital angular momentum³³. However, it is not easy to measure these components of light, particularly in the near-field as would be required here. By optimizing the polarization and the coupling gap, the power of the highest measured peak is 1.8% of the input power. Assuming that the input coupling equals the output coupling, the maximum coupling efficiency to the WGMs should, in principle, exceed 10%. The efficiency could be increased by optimizing the shape of the antenna.

Finally, if we consider that the microsphere resonator can support different azimuthal modes and that Rayleigh scattering need not satisfy the phase-matching condition, it should be possible to achieve coupling over almost the entire surface of the resonator, except for a small region around the support stem. We have experimentally confirmed this (results not presented). This could prove to be particularly convenient when the system is in a noisy environment, where a standard tapered fiber coupling system may not be feasible.

Based on our experimental results presented herein, we propose that the fiber-based optical antenna coupling method is suitable for building an ultracompact whispering gallery resonator-based sensor. The microresonator and the antenna could be packaged together as a minuscule probe, with a lateral size less than 1 mm. Such probes hold promise for producing low-cost, portable, and highly sensitive point-of-care (POC) diagnostic devices.

I. FUNDING INFORMATION

This work was funded by the Okinawa Institute of Science and Technology (OIST) Graduate University.

¹A. B. Matsko and V. S. Ilchenko, IEEE J. Sel. Top. Quantum Electron **12**, 3 (2006).

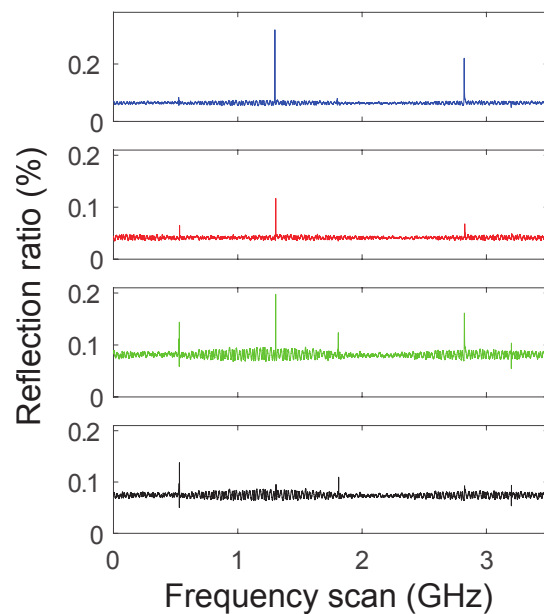


FIG. 3. Reflected spectra for different polarizations. The polarization is changed by rotating PC.

- ²L. He, Ş. K. Özdemir, and L. Yang, Laser & Photon. Reviews **7**, 60 (2013).
- ³F. Lei, Y. Yang, J. M. Ward, and S. Nic Chormaic, Opt. Express **25**, 24679 (2017).
- ⁴G. Lin, A. Coillet, and Y. K. Chembo, Adv. Opt. Photonics **9**, 828 (2017).
- ⁵D. Vernooy, A. Furusawa, N. P. Georgiades, V. Ilchenko, and H. Kimble, Phys. Rev. A **57**, R2293 (1998).
- ⁶F. Lei, R. M. Murphy, J. M. Ward, Y. Yang, and S. Nic Chormaic, Photon. Res. **5**, 362 (2017).
- ⁷M. Aspelmeyer, T. J. Kippenberg, and F. Marquardt, Rev. Mod. Phys. **86**, 1391 (2014).
- ⁸X. Jiang, A. J. Qavi, S. H. Huang, and L. Yang, arXiv preprint arXiv:1805.00062 (2018).
- ⁹J. M. Ward, Y. Yang, F. Lei, X.-C. Yu, Y.-F. Xiao, and S. Nic Chormaic, Optica **5**, 674 (2018).
- ¹⁰B. Peng, Ş. K. Özdemir, F. Lei, F. Monifi, M. Gianfreda, G. L. Long, S. Fan, F. Nori, C. M. Bender, and L. Yang, Nat. Phys. **10**, 394 (2014).
- ¹¹X. Jiang, L. Shao, S.-X. Zhang, X. Yi, J. Wiersig, L. Wang, Q. Gong, M. Lončar, L. Yang, and Y.-F. Xiao, Science **358**, 344 (2017).
- ¹²V. Braginsky, M. Gorodetsky, and V. Ilchenko, Phys. Lett. A **137**, 393 (1989).
- ¹³V. S. Ilchenko, X. S. Yao, and L. Maleki, Opt. Lett. **24**, 723 (1999).
- ¹⁴J. C. Knight, G. Cheung, F. Jacques, and T. Birks, Opt. Lett. **22**, 1129 (1997).
- ¹⁵J. Love, W. Henry, W. Stewart, R. Black, S. Lacroix, and F. Gonthier, IEEE Proceedings J-Optoelectronics **138**, 343 (1991).
- ¹⁶Y.-Z. Yan, C.-L. Zou, S.-B. Yan, F.-W. Sun, Z. Ji, J. Liu, Y.-G. Zhang, L. Wang, C.-Y. Xue, W.-D. Zhang, *et al.*, Opt. Express **19**, 5753 (2011).
- ¹⁷G. Zhao, Ş. K. Özdemir, T. Wang, L. Xu, E. King, G.-L. Long, and L. Yang, Sci. Bull. **62**, 875 (2017).
- ¹⁸P. Wang, R. Madugani, H. Zhao, W. Yang, J. M. Ward, Y. Yang, G. Farrell, G. Brambilla, and S. Nic Chormaic, IEEE Photon. Technol. Lett. **28**, 2277 (2016).
- ¹⁹F.-J. Shu, C.-L. Zou, and F.-W. Sun, Opt. Lett. **37**, 3123 (2012).

- ²⁰Y.-D. Yang, S.-J. Wang, and Y.-Z. Huang, *Opt. Express* **17**, 23010 (2009).
- ²¹S. Liu, W. Sun, Y. Wang, X. Yu, K. Xu, Y. Huang, S. Xiao, and Q. Song, *Optica* **5**, 612 (2018).
- ²²X. Bai and D. Wang, *Opt. Lett.* **43**, 5512 (2018).
- ²³J. Liu, W. Chen, D. Wang, B. Xu, and Z. Wang, *IEEE Photon. Technology Lett.* **30**, 537 (2018).
- ²⁴F. Shu, X. Jiang, G. Zhao, and L. Yang, *Nanophotonics* (2018).
- ²⁵M. Motsch, M. Zeppenfeld, P. W. Pinkse, and G. Rempe, *New J. Phys.* **12**, 063022 (2010).
- ²⁶T. J. Kippenberg, A. Tchebotareva, J. Kalkman, A. Polman, and K. J. Vahala, *Phys. Rev. Lett.* **103**, 027406 (2009).
- ²⁷J. Zhu, Ş. K. Özdemir, H. Yilmaz, B. Peng, M. Dong, M. Tömes, T. Carmon, and L. Yang, *Sci. Rep.* **4**, 6396 (2014).
- ²⁸J. Knight, N. Dubreuil, V. Sandoghdar, J. Hare, V. Lefevre-Seguin, J. Raimond, and S. Haroche, *Opt. Lett.* **20**, 1515 (1995).
- ²⁹S. K. Mondal, A. Mitra, N. Singh, S. Sarkar, and P. Kapur, *Opt. Express* **17**, 19470 (2009).
- ³⁰S. K. Mondal, A. Mitra, N. Singh, F. Shi, and P. Kapur, *IEEE Photon. Tech. Lett.* **23**, 1382 (2011).
- ³¹S. K. Mondal, S. S. Pal, D. Kumbhakar, U. Tiwari, and R. Bhatnagar, *Appl. Opt.* **52**, 5455 (2013).
- ³²M. F. Limonov, M. V. Rybin, A. N. Poddubny, and Y. S. Kivshar, *Nature Photonics* **11**, 543 (2017).
- ³³S. Sarkar Pal, S. Mondal, D. Kumbhakar, R. Kumar, A. Akula, R. Ghosh, and R. Bhatnagar, *Appl. Phys. Lett.* **104**, 031105 (2014).